ResearchGate

See discussions, stats, and author profiles for this publication at: https://www.researchgate.net/publication/223173724

Cationic Bis-cyclometallated Iridium(III) Phenanthroline Complexes with Pendant Fluorenyl Substituents: Synthesis, Redox, Photophysical Properties and Light-Emitting Cells

ARTICLE *in* CHEMISTRY · JANUARY 2008

Impact Factor: 5.73 · DOI: 10.1002/chem.200700308

CITATIONS
61

READS
84

8 AUTHORS, INCLUDING:

M. Tavasli
Uludag University

30 PUBLICATIONS **684** CITATIONS

SEE PROFILE

Igor F Perepichka
Bangor University

125 PUBLICATIONS **3,148** CITATIONS

SEE PROFILE

Chien-Jung Chiang
Durham University

6 PUBLICATIONS **198** CITATIONS

SEE PROFILE

Andy Monkman
Durham University

416 PUBLICATIONS **9,837** CITATIONS

SEE PROFILE

Available from: Andy Monkman
Retrieved on: 27 January 2016

DOI: 10.1002/chem.200700308

Cationic Bis-cyclometallated Iridium(III) Phenanthroline Complexes with Pendant Fluorenyl Substituents: Synthesis, Redox, Photophysical Properties and Light-Emitting Cells

Xianshun Zeng,[a] Mustafa Tavasli,[a] Igor F. Perepichka,[a] Andrei S. Batsanov,[a] Martin R. Bryce,*[a] Chien-Jung Chiang,[b] Carsten Rothe,[b] and Andrew P. Monkman[b]

Abstract: We report the synthesis, characterisation, photophysical and electrochemical properties of a series of cationic cyclometallated Ir^{III} complexes of general formula $[Ir(ppy)_2(phen)]PF_6$ (ppy = 2-phenylpyridine, phen = a substituted phenanthroline). A feature of these complexes is that the phen ligands are substituted with one or two 9,9-dihexylfluorenyl substituents to provide extended π conjugation, for example, the 3-[2-(9,9-dihexylfluorenyl)]-phenanthroline and 3,8-bis[2-(9,9-dihexylfluorenyl)]phenanthroline ligands afford complexes **6** and **9**, respectively. A single-crystal X-ray diffraction study of a related complex **18** containing the 3,8-bis(4-iodophenyl)phenanthroline ligand, revealed an octahedral coordination of the Ir atom, in which the metallated C atoms of the ppy ligands occupy *cis* positions. The complexes **6** and **9** displayed reversible oxidation waves in cyclic voltammetric studies ($E^{ox}_{1/2} = +1.18$ and $+1.20$ V, respectively, versus Ag/Ag^+ in CH_2Cl_2) assigned to the metal-centred Ir^{III}/Ir^{IV} couple. The complexes exhibit strong absorption in the UV region in solution spectra, due to spin-allowed ligand-centred (LC) $^1\pi$–π^* transitions; moderately intense bands occur at approximately 360–390 nm which are red-shifted with increased ligand length. The photoluminescence spectra of all the complexes were characterised by a broad band at $\lambda_{max} \approx 595$ nm assigned to a combination of ^{3}MLCT and $^3\pi \rightarrow \pi^*$ states. The long emission lifetimes (in the microsecond time-scale) are indicative of phosphorescence: the increased ligand conjugation length in complexes **9** and **17** leads to increased lifetimes for the complexes ($\tau = 2.56$ and 2.57 μs in MeCN, respectively) compared to monofluorenyl analogues **6** and **15** ($\tau = 1.43$ and 1.39 μs, respectively). DFT calculations of the geometries and electronic structures of complexes **6′**, **9′** (for both singlet ground state (S_0) and triplet first excited (T_1) states) and **18** have been performed. In the singlet ground state (S_0) HOMO orbitals in the complexes are spread between the Ir atom and benzene rings of the phenylpyridine ligand, whereas the LUMO is mainly located on the phenanthroline ligand. Analysis of orbital localisations for the first excited (T_1) state have been performed and compared with spectroscopic data. Spin-coated light-emitting cells (LECs) have been fabricated with the device structures ITO/PEDOT:PSS/Ir complex/Al, or Ba capped with Al (ITO = indium tin oxide, PEDOT = poly(3,4-ethylenedioxythiophene), PSS = poly(styrene) sulfonate). A maximum brightness efficiency of $9\ cd\,A^{-1}$ has been attained at a bias of 9 V for **17** with a Ba/Al cathode. The devices operated in air with no reduction in efficiency after storage for one week in air.

Keywords: fluorene · N ligands · cyclometalation · iridium · luminescence · organic light-emitting devices

[a] Dr. X. Zeng, Dr. M. Tavasli, Dr. I. F. Perepichka,[+] Dr. A. S. Batsanov, Prof. M. R. Bryce
Department of Chemistry, Durham University
Durham DH1 3LE (UK)
Fax: (+44) 191-384-4737
E-mail: m.r.bryce@durham.ac.uk

[b] C.-J. Chiang, Dr. C. Rothe, Prof. A. P. Monkman
Department of Physics, Durham University
Durham DH1 3LE (UK)

[+] Current address: Centre for Materials Science
Faculty of Science and Technology
University of Central Lancashire, Preston, PR1 2HE (UK)

Supporting information for this article is available on the WWW under http://www.chemistry.org or from the author and includes: general details of instrumentation and procedures; synthetic and characterisation details for all new compounds; crystal structure data for complex **18**; additional absorption and emission spectra; AFM image of complex **17** on a glass/ITO/PEDOT-PSS substrate; EL spectra for complex **9** and luminance and luminous efficiency data for an LEC of **9** as a function of time; atomic coordinates for the geometry optimisations.

 © 2008 Wiley-VCH Verlag GmbH & Co. KGaA, Weinheim

Introduction

Luminescent transition-metal complexes are of great interest as multifunctional chromophores for advanced optoelectronic applications.[1] In particular, a broad selection of ligands, principally based upon 2-phenylpyridine (ppy),[2] have been utilised to form phosphorescent bis-[3] and tris-cyclometallated[4] neutral iridium(III) complexes. The photophysical properties of these phosphors can be tuned by varying the ligand[5] or its substituent groups and by the use of additional ancillary ligands.[6] Complexes of this type are components in electrophosphorescent organic/polymer light-emitting devices (O/PLEDs) where they generally function as an emitting guest in a blend with a host material.[7] The electrogenerated singlet and triplet excited states mix by spin–orbit coupling and all the triplet excited states contribute to light emission. Additionally, the triplet state lifetime is usually shortened, which helps to suppress triplet–triplet annihilation. The key properties of transition-metal complexes are their high stability, high luminescence quantum yields, short excited state lifetime and tuneable emission energy.

Ionic chromophores have attracted attention recently as structural variants of the more widely studied neutral complexes. A selection of heteroleptic charged Ir species comprising two cyclometallating ppy ligands and a neutral diimine ligand (usually 2,2-bipyridine) of generic formula $(C^\wedge N)_2Ir(N^\wedge N)^+X^-$ (typically $X = PF_6$) **1** have been studied.[8] Analogues with different cyclometallating ligands (e.g., 1-phenylpyrazole, benzoquinoline, 2-thienylpyridine and 1-phenylisoquinoline) are also known.[9] The N^N ligand can serve to improve complex stability compared to tris-cyclometallated systems and the presence of counterions may be beneficial for device applications. These counterions are mobile under the influence of an applied bias leading to accumulation of negative ionic charge near one electrode and depletion near the other electrode. This ionic space charge creates high electric fields at the electrodes which increases electronic charge injection into the metal complexes. Thus operating voltages can be quite low and air-stable electrodes can be used.

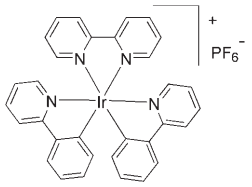

1

The effect on the redox and optoelectronic properties of changing the structure of the ligands (especially the N^N ligand) around a charged Ir centre remains largely unexplored.[10] From this viewpoint, we now describe the synthesis and photophysical properties of the new cationic iridium complexes **6**, **9**, **15** and **17** (Schemes 1–4, respectively), which comprise two cyclometallating C^N ppy ligands and one N^N phenanthroline ligand. Phenanthroline was chosen as a variant to 2,2-bipyridine as it is known to form stable complexes with iridium.[8d,9c,11] 9,9-Dihexylfluorene units were attached to the phenanthroline unit to enhance organic solubility and hydrophobicity and to extend the ligand π system, which should be beneficial in reducing non-radiative intermolecular charge recombination due to steric effects, as recently noted by Bolink and co-workers for an analogous 4,7-diphenylphenanthroline complex.[11d] Additionally, in complexes **15** and **17** carbazole units were attached because of their known high stability, processability and hole-transporting properties.[12] We[13] and others[14] have recently reported the photophysical properties of neutral cyclometallated Ir^{III} complexes which incorporate fluorene units into the ligands. A charged complex has been used by Wong and co-workers as a phosphorescent dopant in a multilayer OLED.[14d]

Results and Discussion

Synthesis of ligands and their iridium complexes: The synthesis of complexes **6** and **9** is shown in Schemes 1 and 2, respectively.

3-Bromo- and 3,8-dibromo-1,10-phenanthroline,[15] **2** and **7**, respectively, were the precursors to the new substituted ligands. For the first series of complexes, the Suzuki–Miyaura cross-coupling reactions[16] with the fluorenylboronic ester **3**[17] proceeded in good yields under standard conditions ($[Pd(PPh_3)_4]$, Na_2CO_3 (aq), toluene, 88 °C) to give the phenanthroline–fluorene conjugates **4** and **8**, respectively. The charged complexes **6** and **9** were then obtained by reaction of these ligands with the dimeric species $[\{Ir(ppy)_2Cl\}_2]$ **5**, followed by anion exchange by using KPF_6, based on literature precedents.[18]

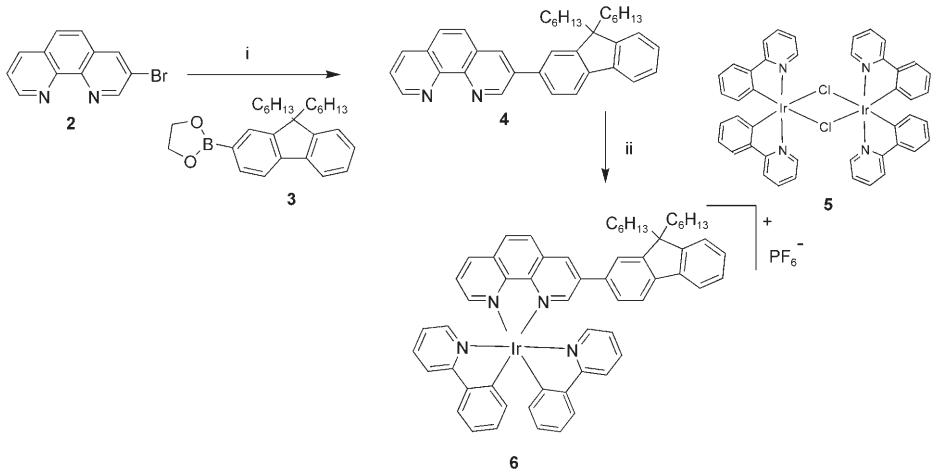

Scheme 1. Reagents and conditions: i) compounds **2**+**3**, $[Pd(PPh_3)_4]$, 1 M Na_2CO_3 (aq), toluene, 88 °C, 72 h (77 % yield); ii) compounds **4**+**5**, CH_2Cl_2, MeOH, reflux, 24 h; then KPF_6, 20 °C, 1 h (73 % yield).

 © 2008 Wiley-VCH Verlag GmbH & Co. KGaA, Weinheim

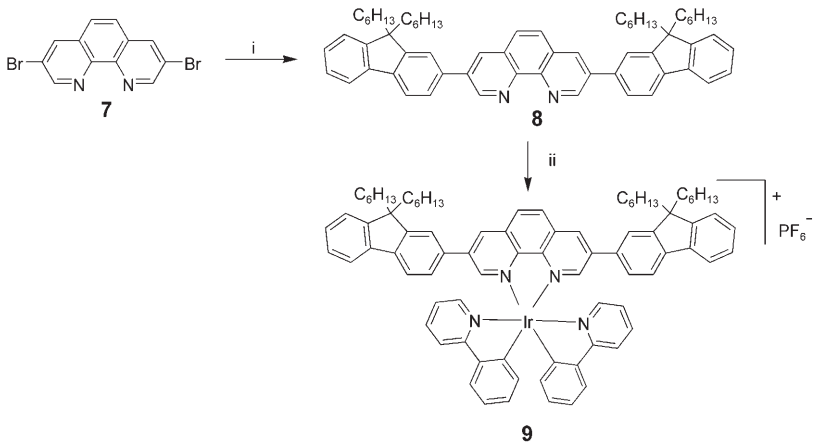

Scheme 2. Reagents and conditions: i) compounds **7** (1 equiv), **3** (2.0 equiv), $[Pd(PPh_3)_4]$, 1 M Na_2CO_3 (aq), toluene, 88 °C, 48 h (77 % yield); ii) compounds **8** (0.1 equiv), **5** (0.05 equiv), CH_2Cl_2, MeOH, reflux, 24 h; then KPF_6, 20 °C, 1 h (90 % yield).

The second series of ligands **14** and **16** and their complexes **15** and **17** (Schemes 3 and 4) have pendant carbazole units which were attached to the fluorene unit by twofold alkylation at the C9 position of 2-iodofluorene **10** by using *N*-(6-bromohexyl)carbazole **11** under basic conditions to afford **12** in 88 % yield. Compound **12** was then converted to the boronic ester derivative **13** in 71 % yield. The phenanthroline ligands **14** and **16** were subsequently obtained from **13**, by analogy with reactions of **3** shown in Schemes 1 and 2.

Crystal structure of complex 18: None of the complexes **6**, **9**, **15** or **17** gave crystals suitable for X-ray structure analysis. However, the crystal structure of the related complex **18** was determined to confirm the mode of coordination of the phenylpyridine and phenanthroline ligands in this series. The synthesis of **18** is described in the Supporting Information.

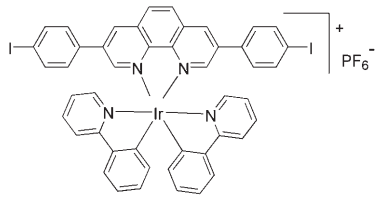

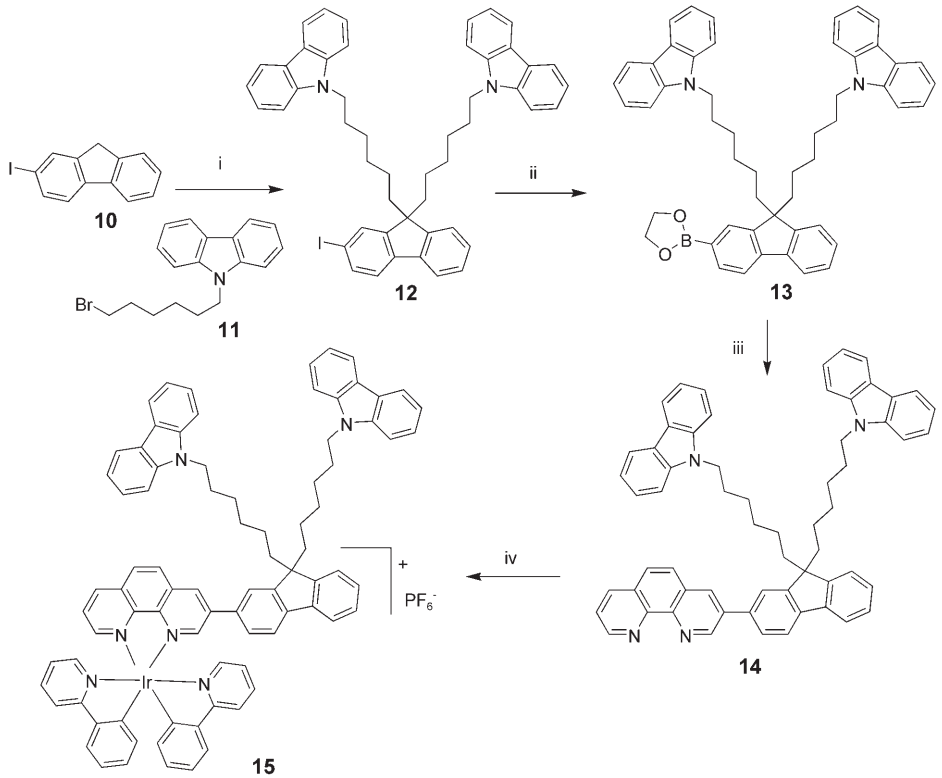

Scheme 3. Reagents and conditions: i) compounds **10**+**11**, NaOH (aq), THF, [18]crown-6, reflux, 36 h (88 % yield); ii) compound **12**, *n*BuLi, THF, −78 °C, 5 h; then $B(OMe)_3$, −78→20 °C, 16 h (71 % yield); iii) compounds **13**+**7**, $[Pd(PPh_3)_4]$, 1 M Na_2CO_3 (aq), THF, toluene, 88 °C, 72 h (79 % yield); iv) compounds **14**+**5**, CH_2Cl_2, MeOH, reflux, 24 h; then KPF_6, 20 °C, 1 h (81 % yield).

The asymmetric unit comprises one complex cation, one-hexafluorophosphate anion (Figure 1) and two acetone molecules (not shown), one of which forms a short O1···I1 contact of 3.27(1) Å and the other is chaotically disordered. The coordination geometry of iridium is similar to that found in previously studied diamino-bis(phenylpyridine)iridium(III) type cations, where the diamino ligands were various bipyridine derivatives[8c,e,19,20] and dipyrido[3,2-*a*:2′,3′-*c*]phenazine (dppz).[21] To our knowledge, no 1,10-phenanthroline complex of this type has been characterised crystallographically. The Ir atom in **18** adopts a distorted octahedral coordination. As usual, the two Ir–C bonds are *cis* to each other and *trans* to the Ir–N(phen) bonds, which are longer than the mutually *trans* Ir–N(ppy) bonds by more than 0.1 Å, due to a *trans* influence. In bipyridine-bis(phenyl-

 © 2008 Wiley-VCH Verlag GmbH & Co. KGaA, Weinheim

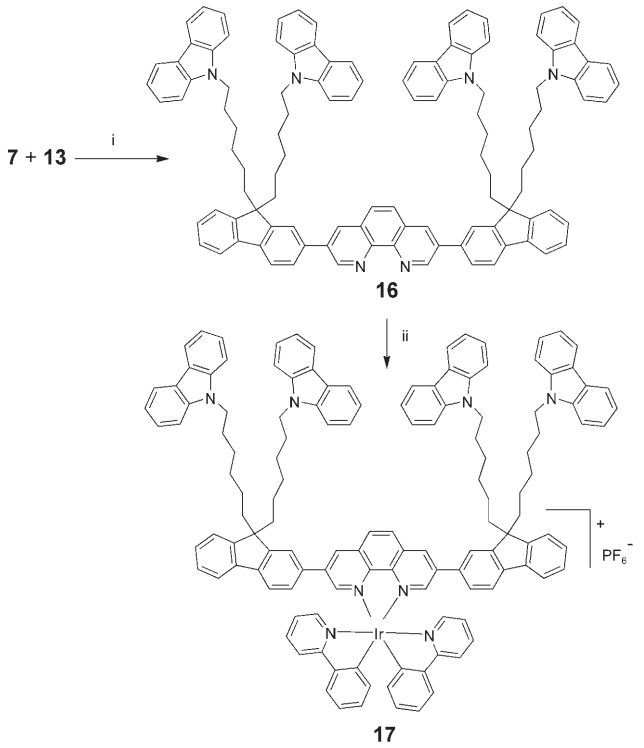

Scheme 4. Reagents and conditions: i) compounds **7+13** (2 equiv), [Pd(PPh$_3$)$_4$], 1 M Na_2CO_3 (aq), THF, toluene, 88 °C, 48 h (84 % yield); ii) compounds **16+5**, CH_2Cl_2, MeOH, reflux, 24 h; then KPF_6, 20 °C, 1 h (92 % yield).

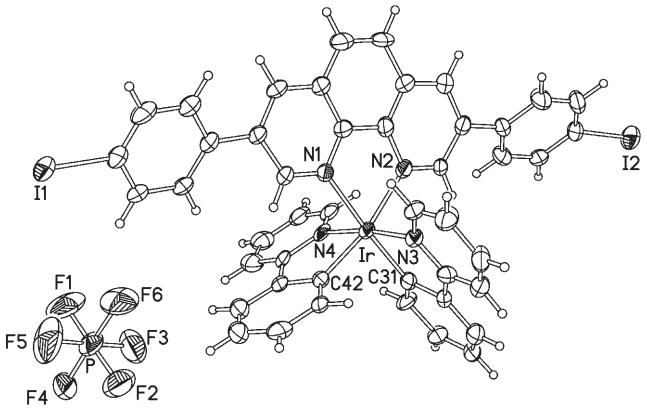

Figure 1. Cation and anion in the crystal of **18**·2Me$_2$CO (50 % probability thermal ellipsoids).

pyridine) complexes the Ir–C distances of 1.99–2.04 and Ir–N(ppy) distances of 2.04–2.06 Å are similar, whereas the Ir–N(bpy) distances are 2.12–2.16 Å in sterically unhindered complexes, but may increase to 2.22–2.26 Å for 2,9-substituted bpy ligands. Interestingly, the dppz complex[21] shows a uniform lengthening of Ir–C, Ir–N(ppy) and Ir–N(dppz) bonds, averaging 2.07(2), 2.10(2) and 2.17(2) Å, respectively, although the precision of the latter structure is not high. The bpy ligand has substantial conformational flexibility;[22] in the complexes mentioned above it is twisted around the central C–C bond by up to 10° (and in the case of 2,9-diphenyl-4,7-di-*tert*-butylbipyridine ligand,[8c] by as much as 33°). Clearly, phenanthroline (and dppz) ligands lack this flexibility. Possibly for this reason, the phenanthroline ligand "bite" angle (N-Ir-N) in **18** is somewhat wider than those typical for bpy ligands (75.2–76.7°), although it remains smaller than the N-Ir-C "bite" angles of the ppy ligands.

Solution electrochemical studies: Cyclic voltammetric (CV) studies of iridium complexes were carried out in dichloromethane solution with 0.1 M tetra-*n*-butylammonium hexafluorophosphate (Bu_4NPF_6) as the supporting electrolyte. The oxidation potentials of the complexes **6**, **9**, **15** and **17** and ferrocene as an internal reference (Fc/Fc$^+$ couple: $E^{ox}_{1/2}=+0.46$ V versus SCE[23]) versus Ag/Ag$^+$ are summarised in Table 1 and the CV traces are shown in Figure 2. The

Table 1. Summary of the half-wave oxidation potentials ($E^{ox}_{1/2}$ [V]) obtained by cyclic voltammetry for complexes **6**, **9**, **15**, **17**, *N*-hexylcarbazole and ferrocene versus Ag/Ag$^+$.[a]

Compound	$E^{ox}_{1/2}$ {E^{ox}_{pa}, E^{ox}_{pc}} [ΔE, mV] versus Ag/Ag$^+$
6	+1.18 [75]
9	+1.20 [76]
15	{1.06, 0.98}
17	1) {1.06, 0.57} 2) 1.08[94]
N-hexylcarbazole	{1.05, 0.67}
ferrocene	0.28 [65]

[a] 0.1 M Bu_4NPF_6 in dichloromethane, scan rate = 100 mV s^{-1}.

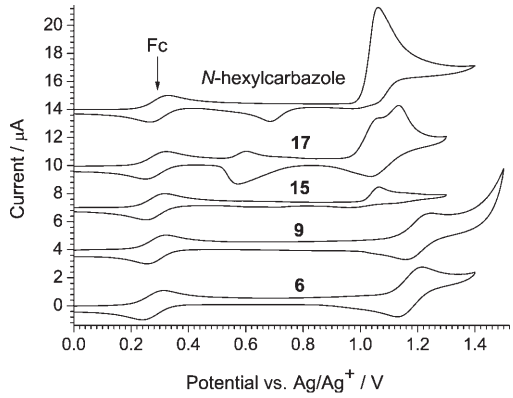

Figure 2. Cyclic voltammograms of complexes **6**, **9**, **15**, **17** and *N*-hexylcarbazole in a solution of 0.1 M Bu_4NPF_6 dichloromethane, scan rate 100 mV s^{-1}, with ferrocene (Fc) as an internal reference.

CV traces of the complexes **6** and **9** both displayed chemically reversible oxidation waves (at $E^{ox}_{1/2}=+1.18$ and +1.20 V, respectively). The increase in the ligand length by one fluorene unit (from **6** to **9**) produced only a small effect (20 mV positive shift) on the oxidation potential of **9** which is understandable from DFT calculations, according to which the HOMO energies of both complexes are close, and HOMO orbitals are spread between the iridium atom and benzene rings of ppy ligands, with no coefficients on the fluorene-phenathroline ligand (see theoretical section below).

 © 2008 Wiley-VCH Verlag GmbH & Co. KGaA, Weinheim

Only a minor effect of the structure of the phenanthroline ligand on the oxidation potentials of its iridium complexes has been observed before,[9a] which is understandable as the oxidation processes are mostly associated with the bis-cyclometallated phenyl-Ir moiety and therefore are assigned to the pure metal-centred Ir^{III}/Ir^{IV} couple.[24] The CVs of the carbazole-containing complexes **15** and **17** are different from complexes **6** and **9** and more complicated. They exhibit irreversible oxidation waves in which the anodic peaks are dominated by the E_{pa} of the *N*-hexylcarbazole unit which occurs at +1.05 V. Carbazoles, such as 1,4-bis(carbazolyl)-benzene ($E_{pa}^{ox}=+1.04$ V)[25] are known to have irreversible oxidation potentials. This irreversibility would explain the re-reduction cathodic peak (E_{pc}^{ox}) observed at +0.67 V for *N*-hexylcarbazole and at +0.57 V for **17**. This process overlaps the second quasi-reversible oxidation process in **15** and **17**, which is assigned to a metal-centred Ir^{III}/Ir^{IV} couple.

Solution-state photophysical properties

Absorption: The absorption spectra of ligands **4**, **8**, **14** and **16** in toluene show a red shift for the bifluorene derivatives **8** and **16** ($\lambda_{max}=347$ nm) compared to the monofluorene analogues **4** and **14** ($\lambda_{max}=330$ nm) (see Supporting Information, Figure S1). The absorption spectra of complexes **6**, **9**, **15** and **17** were recorded both in toluene (Figure 3) and in acetonitrile solution (see Supporting Information, Figure S2). In acetonitrile all of these complexes showed intense peaks below $\lambda=300$ nm, which are hidden in toluene by the solvent cut-off, and are assigned to spin-allowed $^1\pi$–π^* intraligand (^{1}IL, C^N and N^N) transitions. At $\lambda>$ 300 nm, both in toluene and acetonitrile, less intense absorption features were seen. First, at around $\lambda=340$ nm two well-resolved absorption peaks were observed in complexes **15** and **17**, and were attributed to the presence of the carbazole units. Second, broad absorption bands at $\lambda\approx360$ nm were observed for complexes **6** and **15**, and were shifted to the red (ca. 390 nm) in complexes **9** and **17** with the increase in the ligand length. This red shift is similar to the absorption of charged iridium complexes containing poly(9,9-dioctylfluorene)[26] and also the increase in the extinction coefficients with increased conjugation length indicates that this region (from 360 to 450 nm) is mainly dominated by the ligand $S_1\leftarrow S_0$ transitions. This absorption region shows a minor solvatochromic shift to shorter wavelengths with increased solvent polarity, for example, λ_{max} for complexes **9** and **17** are 387 and 390 nm, respectively (in toluene) and 380 nm (in acetonitrile). Finally, as evident from their low energy and low extinction coefficients, the weak bands at around 400 nm and those extending towards the red are assigned to both spin-allowed metal-to-ligand charge-transfer (^{1}MLCT) transitions ($\varepsilon\approx(1–2)\times10^4\,M^{-1}\,cm^{-1}$) and spin–orbit-coupling-enhanced ^{3}LC and ^{3}MLCT transitions (shoulders at 468 nm, with $\varepsilon\approx(1–2)\times10^3\,M^{-1}\,cm^{-1}$). These features are consistent with the literature data for related iridium complexes.[19] It is also noteworthy that extinction coefficients increased as the conjugation length increased. However, the increase for the carbazole-containing complexes (e.g., from **15** to **17**) was less pronounced than the increase from **6** to **9**.

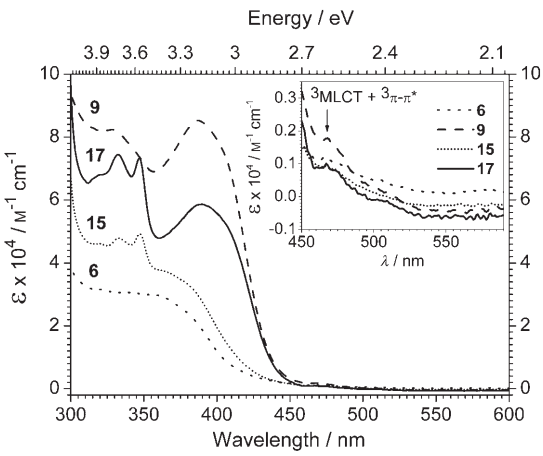

Figure 3. The absorption spectra for complexes **6**, **9**, **15** and **17** in toluene. Inset: expansion of the 450–600 nm region.

Emission: The photoluminescence (PL) spectra of complexes **6**, **9**, **15** and **17** obtained from degassed solutions in toluene at room temperature (excitation at 390 nm) are shown in Figure 4. The increase in the emission intensities upon degassing, even though spectral profiles remained unchanged, indicated the presence of long-lived phosphorescent species which are susceptible to oxygen quenching.[4,14a] The PL spectra of all complexes are characterised by a broad and structureless emission spectrum centred around $\lambda_{max}\approx595$ nm. An increase in conjugation length of the phenanthroline ligand from one fluorene unit in **6** and **15** to two in **9** and **17** shifted the emission maximum to the red (by only 5 nm). A similar effect has been previously reporte-

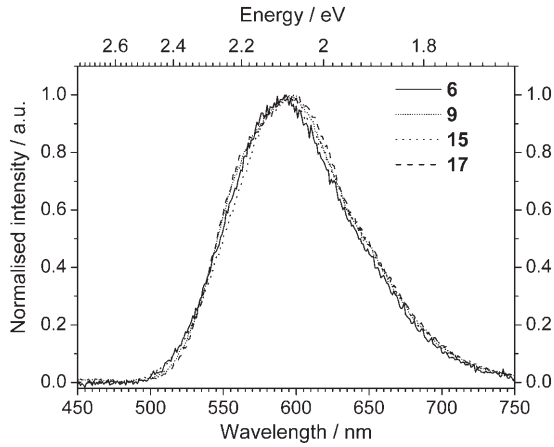

Figure 4. Normalised photoluminescence (PL) spectra for complexes **6**, **9**, **15** and **17** in degassed toluene, excited at 390 nm.

 © 2008 Wiley-VCH Verlag GmbH & Co. KGaA, Weinheim

d[13a,c,14c] as the conjugation length increased. However, when compared with the parent complex, $(ppy)_2Ir(phen)^+$ (λ_{max}^{PL} = 579 nm, ppy = 2-phenylpyridine, phen = 1,10-phenanthroline)[8d] significant red shifts were observed (15 nm for **6** and **15**, 20 nm for **9** and **17**, respectively) consistent with extended conjugation involving the π systems of the phenanthroline and fluorene units. Red shifts in emission maxima were also observed by Zhao and co-workers[9b] with increasing conjugation length of diimine ligands. The PL spectra of the complexes in degassed acetonitrile solutions were also investigated (see Supporting Information, Figure S2) and a blue shift (7–10 nm) in the emission maxima (586 nm) was observed for **9** and **17**, compared to those of **6** and **15**, respectively.

A red shift (15–20 nm) in emission and also a large Stokes' shift (125 nm)[7b] between λ_{max} for ^{3}MLCT absorption and emission spectra may indicate that the intraligand (^{3}IL) $^3\pi\rightarrow\pi^*$ state contributes to the emission. Given the broad and structureless characteristics of the emission spectra, the sensitivity to the medium and the relatively long lifetimes observed (in the microsecond time scale; see below), ^{3}MLCT states also contribute to the emission. Hence it can be concluded that the emission originates from mixed ^{3}MLCT/$^3\pi\rightarrow\pi^*$ states. This is in agreement with an observation by Lowry and co-workers[9c] that a library of iridium complexes containing both cyclometallating and aromatic diimine ligands had emissions from mixed excited states.

Theoretical studies: The geometries and electronic structures of complexes **6**, **9** and **18** were calculated by using the density functional theory (DFT) method at the B3LYP/(6-31G(d,p)+LANL2DZ) level. To decrease the computation time calculations were performed for analogues of **6** and **9**, in which CH_3 substituents replaced the C_6H_{13} chains (denoted as **6′** and **9′**, respectively). The geometries of both the singlet ground state (S_0) and the lowest triplet state (T_1) were fully optimised without imposing any symmetry restriction and constraints. Selected bond lengths and angles involving the Ir atom are given in Table 2, together with X-ray diffraction data for **18**. DFT calculations for a gas-phase structure correspond well with the Ir–C bond lengths observed in a crystal of solvate **18**·2Me_2CO, whereas the calculated Ir–N lengths are somewhat longer (by ≈0.03–0.04 Å for Ir–N(3,4) and ≈0.07 Å for Ir–CN(1,2) Table 2). All compounds adopt a geometry with orthogonal bonds between the Ir atom and the carbon atoms of ppy ligands (C3-Ir-C4 close to 90°), whereas C–N bonds between the Ir and nitrogen atoms of the ppy ligands form N3-Ir-N4 angles close to 180° (Table 2).

When the geometries of the ground state (S_0) and the lowest excited state (T_1) are compared, relatively small geometry changes are observed. In the T_1 state, slight shortening of Ir–N distances is observed, compared to the singlet ground state (S_0), whereas Ir–C bond lengths and C-Ir-C and N-Ir-N angles remain almost unchanged. The benzene

Phosphorescence lifetimes and photoluminescence quantum yields: Time-resolved luminescence decay measurements for all complexes were performed at 298 K in degassed solutions in acetonitrile (OD < 0.7 at λ_{ex} = 355 nm). The phosphorescence decays collected at the emission maximum for each complex show first-order kinetics, with decay times of τ = 1.34 (**6**), 2.56 (**9**), 1.39 (**15**) and 2.76 μs (**17**). The increase in the ligand conjugation length in complexes **9** and **17** clearly induces an increased phosphorescence lifetime of the complexes.

Phosphorescent quantum yields (Φ_{PL}) were measured at room temperature in thoroughly degassed toluene solutions (OD ≈ 0.1)[27] by using $Ir(ppy)_3$ (Φ_{PL} = 0.40 in toluene)[28] as the standard. The Φ_{PL} for the complexes also show a modest increase with the ligand conjugation length from 0.08 (**6** and **15**) to 0.11 (**9** and **17**).

Table 2. Selected bond lengths and angles for complexes **6′**, **9′**, and **18** from DFT B3LYP/(6-31G(d,p)+LANL2DZ) calculations and from X-ray crystallography (for **18**).

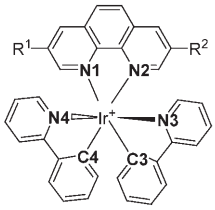

18, R^1 = R^2 = 4-iodophenyl
6', R^1 = H; R^2 = (9,9-dimethyl)fluoren-2-yl
9', R^1 = R^2 = (9,9-dimethyl)fluoren-2-yl

Compound (state)[a]	Bond length [Å]					
	Ir–N1	Ir–N2	Ir–N3	Ir–N4	Ir–C3	Ir–C4
18, X-ray	2.153(6)	2.153(7)	2.051(7)	2.044(6)	2.013(8)	1.995(8)
18 (S_0)	2.228	2.228	2.084	2.083	2.021	2.021
6′ (S_0)	2.226	2.227	2.082	2.084	2.021	2.021
9′ (S_0)	2.227	2.227	2.082	2.082	2.021	2.021
6′ (T_1)	2.214	2.210	2.080	2.079	2.023	2.021
9′ (T_1)	2.208	2.208	2.078	2.078	2.020	2.020

Compound (state)[a]	Angles [°]			Dihedral angles in ppy ligand [°]	
	C3-Ir-C4	N3-Ir-N4	N1-Ir-N2	C3-C-C-N3	C4-C-C-N4
18, X-ray	91.0(3)	172.4(3)	77.5(3)	2(1)	6(1)
18 (S_0)	90.4	173.6	75.6	1.3	1.5
6′ (S_0)	90.5	173.6	75.6	−1.3	−1.4
9′ (S_0)	90.7	173.6	75.7	−1.3	−1.3
6′ (T_1)	90.7	174.1	76.4	−0.7	−1.5
9′ (T_1)	91.2	174.5	76.5	−1.2	−1.2

[a] The geometries of complexes **6′** and **9′** were optimised at both the singlet ground state (S_0) and the lowest triplet state (T_1). The S_0 state was more stable in both cases.

 © 2008 Wiley-VCH Verlag GmbH & Co. KGaA, Weinheim

and pyridine rings in the ppy ligands are essentially coplanar in both S_0 and T_1 states (Table 2).

Figure 5 shows the atomic orbital composition calculated for the frontier molecular orbitals of complexes **6′** and **9′** in the S_0 state. For both complexes the HOMOs (that is, the orbitals into which holes are injected, and which are involved in the hole transport process in light-emitting electrochemical cell (LEC) operation; see below) are distributed between the Ir atom and the benzene rings of the ppy ligands. The LUMOs (the orbitals into which electrons are injected and transported in the LEC) are mainly located on the pyridine rings of the phenanthroline ligand, with only minor extension to the outer fluorene moieties. Extension of the conjugation length (**6′**→**9′**) results in a decrease of both HOMO and LUMO orbital energies (by 0.14 and 0.18 eV, respectively) with only a minor decrease in the HOMO–LUMO gap (0.04 eV). The location of the frontier orbitals in both **6′** and **9′** supports the HOMO–LUMO transition being a mixture of ^{1}MLCT and ligand-to-ligand charge transfer states.

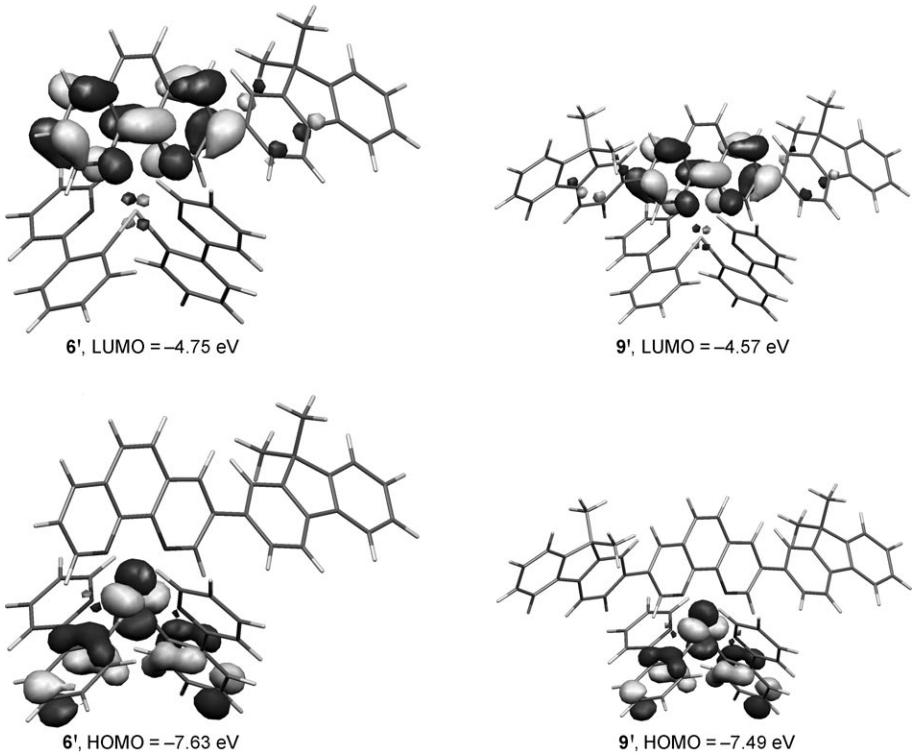

Figure 5. Isocontour plots (0.04 e bohr^{-3}) calculated for the HOMO and the LUMO orbitals of complexes **6′** and **9′**.

The energy difference between T_1 and S_0 at the optimised geometries is calculated to be similar for both complexes (2.23 eV (554 nm) for **6′** and 2.19 eV (565 nm) for **9′**). These values are somewhat blue-shifted compared to the observed emission maxima of the complexes (592 and 596 nm in toluene; and 585 and 584 nm in acetonitrile, for **6** and **9**, respectively; Figure 4 and Figure S3 in the Supporting Information). When the vertical energy difference between T_1 and S_0 is calculated at the optimised geometry of T_1 (by analogy to ref. [11d]) the values (1.76 eV (702 nm) for **6′** and 1.85 eV (670 nm) for **9′**) correspond better to the red edges of the emission rather to their maxima (Figure 4).

Examination of the change in the total charge distribution between the iridium atom and ligands in complexes **6′** and **9′** from the S_0 ground state to the first excited T_1 state is summarised in Table 3. In both cases the positive charge on the Ir centre remains almost constant (with only minor increase by about +0.03–0.05), which indicates that the excited state has little MLCT character. Similar small changes in the charges on the ligands are observed. The overall charges on the two ppy ligands increase in negative charge (by about −0.04–0.02) whereas the positive charge on the phen/Fl ligand (Fl = fluorene) is increased by +0.02–0.03, indicating a net transfer of electron density between the ppy and phen/Fl ligands.

An orbital energy diagram for the triplets (T_1) of **6′** and **9′** is shown in Figure 6 and localisation of the orbitals is shown in Figure 7. For both complexes the higher single occupied orbital (*h*-SOMO) is delocalised between the phenanthroline and fluorene moieties, with larger coefficients on the fluorene compared to that for the LUMO orbitals in the S_0 state (compare Figures 5 and 7). There is a difference in the distribution of occupied orbitals (HOMO, HOMO-1, HOMO-2) and *l*-SOMO between **6′** and **9′**. Whereas **6′** shows a large energy difference for the *l*-SOMO and HOMO(α) orbitals

Table 3. Comparison of charges[a] on iridium atom and ligands in complexes **6′** and **9′** for optimised geometries of the singlet (S_0) and triplet (T_1) states.

Compound (state)[b]	Charge on the fragment			
	Ir	ppy	ppy	phen/Fl
6′ (S_0)	+0.792	−0.135	−0.138	+0.481
6′ (T_1)	+0.820	−0.150	−0.164	+0.495
6′ (S_0^{T1})	+0.826	−0.129	−0.157	+0.495
9′ (S_0)	+0.795	−0.144	−0.144	+0.494
9′ (T_1)	+0.844	−0.152	−0.152	+0.461
9′ (S_0^{T1})	+0.863	−0.172	−0.172	+0.480

[a] Mulliken atomic charges have been used in analysis. [b] S_0 and T_1 are for optimised geometries, S_0^{T1} is for singlet state at T_1-optimised geometry.

 © 2008 Wiley-VCH Verlag GmbH & Co. KGaA, Weinheim

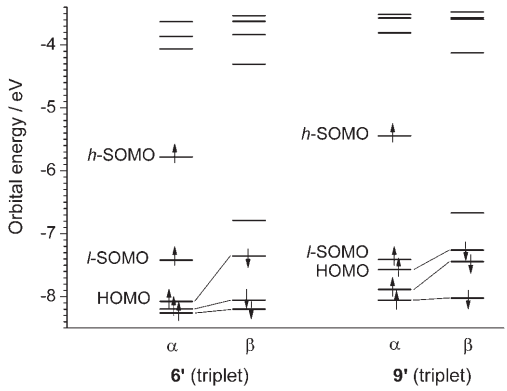

Figure 6. Orbital energy diagram for triplet states of complexes **6′** and **9′** from UB3LYP/(6-31G(d,p)+LANL2DZ) calculations (T_1-optimised geometries).

of 0.65 eV, these orbitals are quite close in energy (0.16 eV difference) in **9′** (Figure 6). This results in a different localisation of orbital coefficients for these complexes. In **6′** *l*-SOMO is mainly localised on the fluorene moiety of the phen/Fl ligand and HOMO(α) is spread between the Ir atom and the benzene rings of two ppy ligands. The reverse situation is observed for **9′**: *l*-SOMO is spread between the Ir atom and the benzene rings of two ppy ligands, whereas HOMO(α) is localised on the fluorene moiety of the phen/Fl ligand (Figure 7).

The DFT calculations suggest possible further design features for this class of Ir complexes for LEC applications. Considering the electron-rich character of the fluorene moiety compared to phenanthroline (in the phen/Fl ligand), and consequently the localisation of the LUMO in the S_0 state predominantly on the phen ring, it would be interesting to study phen ligands with electron-deficient end groups on which the LUMO orbital can be delocalised. The same is valid when considering the localisation of *l*-SOMO orbitals in the first excited T_1 state. Introduction of electron-deficient substituents in the benzene rings of ppy ligands should increase the HOMO coefficients on the Ir centre, thus increasing the contribution of MLCT compared to LLCT transitions.

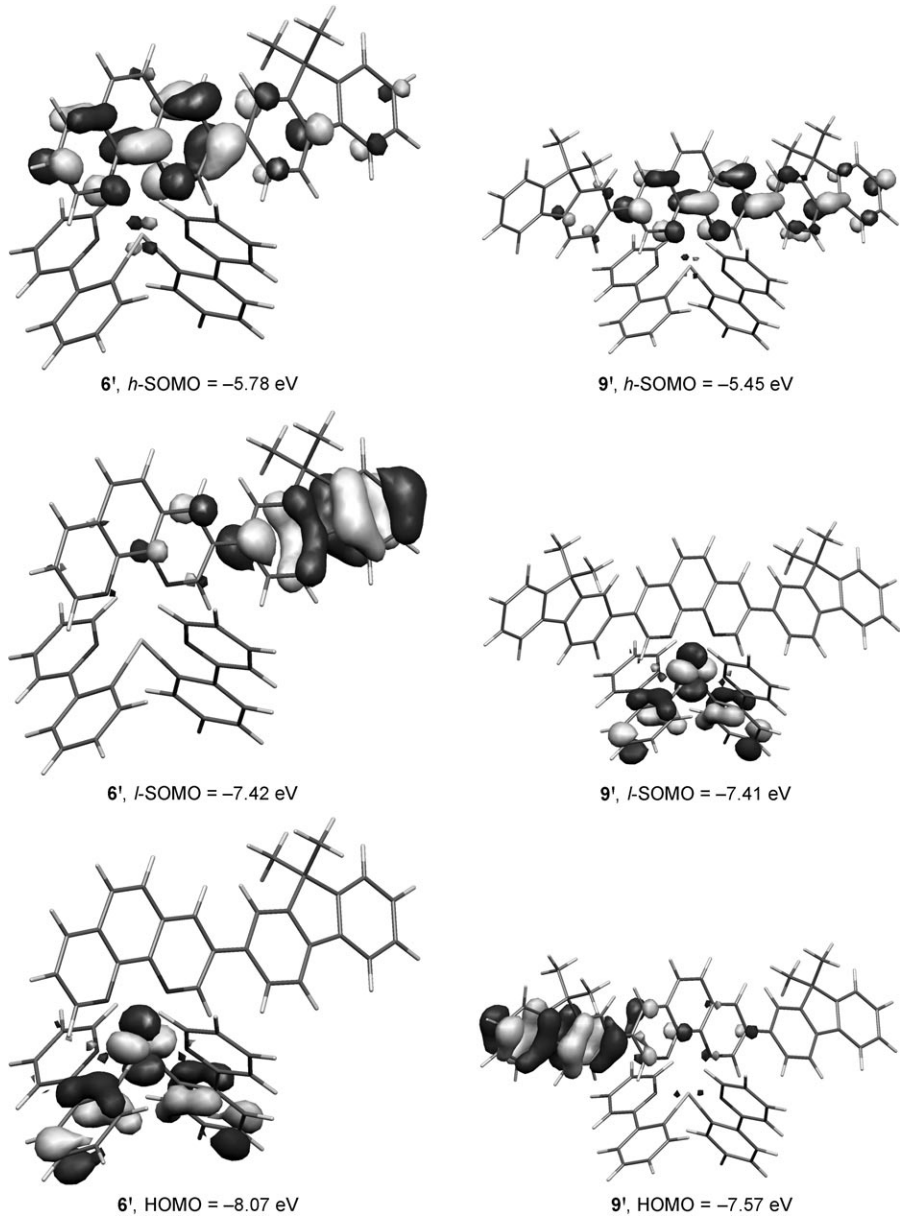

Figure 7. Isocontours plots (0.04 e bohr^{-3}) of higher and lower singly occupied molecular orbitals (*h*-SOMO and *l*-SOMO) and HOMO (α electrons) orbitals for T_1 equilibrium geometries of complexes **6′** and **9′**.

Light-emitting cells (LECs): Spin-coated LECs have been prepared from the iridium complexes **6**, **9**, **15** and **17** with the following device structures: ITO/PEDOT:PSS/Ir complex/Al, or Ba capped with Al (ITO = indium tin oxide, PEDOT = poly(3,4-ethylenedioxythiophene), PSS = poly(styrene) sulfonate). Further details are given in the Supporting Information. Broadly similar results were obtained for all the complexes, the highest efficiencies were obtained for **17** and these data are presented below. Analogous data for an LEC made from **9** are shown in the Supporting Information, Figures S5 and S6. An AFM image of a film of complex **17** spin-coated from a solution in toluene is shown in the Sup-

 © 2008 Wiley-VCH Verlag GmbH & Co. KGaA, Weinheim

porting Information (Figure S4). With <1 nm deviation, the average surface roughness is extremely low for a spin-coated organic material. It is notable that the solubilising substituents enable such good quality films to be obtained from a solution in toluene, rather than the more polar and commonly used acetonitrile. Microcrystallites of complex **17** can be seen as regular needles, of approximately 15 nm length, positioned perpendicular to the film surface.

Figure 8 compares the thin film PL and the electroluminescence (EL) spectra of an LEC made from **17**. The EL is

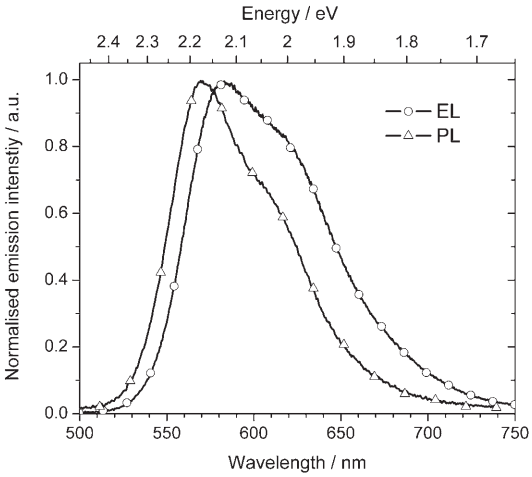

Figure 8. Comparison of solid-state photoluminescence (excitation wavelength 355 nm) and electroluminescence spectra of complex **17** in the device configuration ITO/PEDOT:PSS/**17**/Al.

red-shifted to $\lambda_{max}=570$ nm (2.17 eV) compared to $[Ir(ppy)_3]$ (540 nm, 2.4 eV). The EL of **17** is 40 meV red-shifted compared to the PL, which may be explained by charge trapping and subsequent recombination at sites which are lower in energy. Very similar spectra were obtained for complexes **6**, **9** and **15**, consistent with substitution at the phenanthroline unit having little effect on the HOMO and the LUMO levels of the complexes, which is consistent with recent DFT calculations by Tamayo and co-workers.[9a] Identical spectra were obtained by using Ba/Al as the cathode (data not shown) instead of Al only. It is notable that the thin-film emission spectra are blue-shifted and better resolved than the solution spectra (compare Figures 4 and 8). In solution, the excited state of the complex, with its charge transfer character, can be stabilised leading to broader and typically red-shifted spectra, with longer lifetimes observed in more polar solvents.

Figure 9 shows the typical increase in brightness and brightness efficiency as a function of time for a standard LEC made from **17** and an aluminium cathode. The observed time dependence reflects the diffusion of the PF_6^- counter ions through the film under the applied voltage. In this particular case, about 40 minutes was needed to attain the maximum brightness efficiency of 8 cd A^{-1} by applying a high bias of 9 V; lower voltages are typically used in the lit-

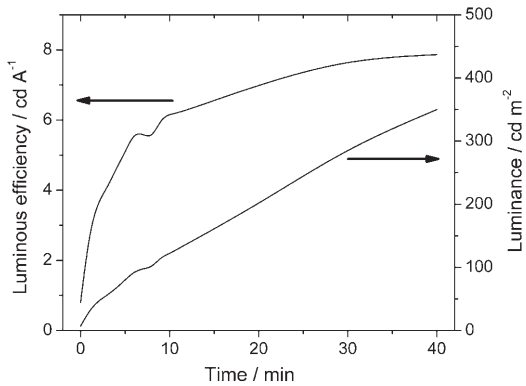

Figure 9. Luminance and luminous efficiency of an ITO/PEDOT:PSS/**17**/Al LEC as a function of time at a bias of 9 V.

erature.[11d] On applying up to 4 V bias no emission was observed from our devices even after several hours. Additionally, when the diode was charged at a high bias and subsequently operated at 3–5 V no current flow was observed and hence no emission was detected. Thus we conclude that the bulky side groups obstruct the diffusion of the counterions and it therefore takes longer to switch on the devices made with the larger complexes. Once charged these devices require a higher bias voltage due to reduced charge mobility. Furthermore, the bias needed to charge and drive our LECs increased with the size and the number of the side chains. The monofluorene complex **6** initially exhibits a higher current which relatively slowly increases with time. In contrast, the current of the more bulky difluorene complex **9** starts from a lower value, but increases more steeply.

Figure 10 shows the maximum brightness that can be reached with LECs of **17** at reasonable efficiencies. To

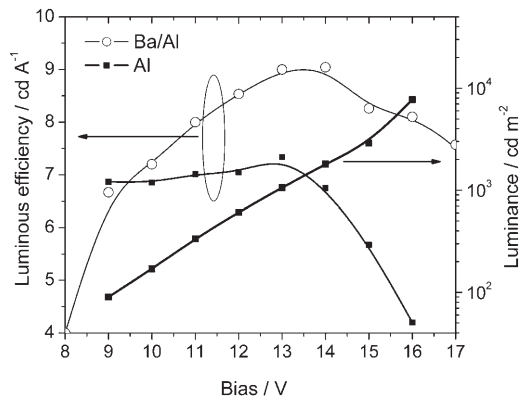

Figure 10. Luminance and luminous efficiency of ITO/PEDOT:PSS/**17**/Al and Ba/Al LECs as a function of bias; data were taken immediately after charging the devices for 20 min at 10 V.

obtain these data the diode was first charged and then tested as a function of bias. By using an aluminium cathode at approximately 14 V less than 1000 cd m^{-2} was achieved with a brightness efficiency of 7 cd A^{-1}. These devices were tested in air without any hermetic sealing. The brightness ef-

 © 2008 Wiley-VCH Verlag GmbH & Co. KGaA, Weinheim

ficiency was further increased to 9 cd A^{-1} by using Ba/Al instead of Al as the cathode, which proves that the electron injection of the Al devices is not ohmic and that the charge carrier balance can be modified to give further improvements in device efficiency. The devices shown in Figure 10 operated in air with no reduction in efficiency after storage for one week in air.

Conclusion

Ionic cyclometallated Ir^{III} complexes of general formula $[Ir(ppy)_2(phen)]^+PF_6^-$ (ppy = 2-phenylpyridine, phen = a substituted phenanthroline) have been synthesised. The phen ligands are substituted with one or two 9,9-dihexylfluorenyl substituents to provide extended π conjugation. The complexes **6** and **9** displayed reversible waves in cyclic voltammetric studies assigned to the metal-centred Ir^{III}/Ir^{IV} couple ($E^{ox}_{1/2} = +1.18$ and $+1.20$ V, respectively, versus Ag/Ag^+ in CH_2Cl_2). The photoluminescence spectra of all the complexes were characterised by a broad band at $\lambda_{max} \approx 595$ nm assigned to a combination of ^{3}MLCT and $^3\pi \rightarrow \pi^*$ states. The increased ligand conjugation length in complexes **9** and **17** leads to increased phosphorescence lifetimes for the complexes ($\tau = 2.56$ and 2.57 μs in MeCN, respectively) compared to monofluorenyl analogues **6** and **15** ($\tau = 1.43$ and 1.39 μs, respectively). DFT calculations have established that in the singlet ground state (S_0) HOMO orbitals in the complexes are spread between the Ir atom and benzene rings of the phenylpyridine ligand, whereas the LUMO is mainly located on the phenanthroline ligand. Analysis of orbital localisations for the first excited (T_1) state have been performed, and compared with spectroscopic data. These complexes possess very good solubility even in non-polar organic solvents and good film-forming properties. Spin-coated light-emitting cells (LECs) with structures ITO/PEDOT:PSS/Ir complex/Al, or Ba capped with Al attain a maximum brightness efficiency of 9 cd A^{-1} at a bias of 9 V for **17** with a Ba/Al cathode. The bias needed to charge and drive our LECs increased with the size and the number of the side chains. The devices operated in air with no reduction in efficiency after storage for one week in air. Further structural modifications to this series of complexes will be reported in due course. These are challenging targets with potentially high rewards in electroluminescent device technology.

Acknowledgements

We thank Durham County Council (Project SP/082), CENAMPS and the University of Durham Photonic Materials Institute for funding this work.

[1] a) J. Slinker, D. Bernards, P. L. Houston, H. D. Abruña, S. Bernhard, G. G. Malliaras, *Chem. Commun.* **2003**, 2392–2399; b) D. Song, S. Wang, *Eur. J. Inorg. Chem.* **2003**, 3774–3782.

[2] V. V. Grushin, N. Herron, D. D. LeCloux, W. J. Marshall, V. A. Petrov, Y. Wang, *Chem. Commun.* **2001**, 1494–1495.

[3] a) S. Lamansky, P. I. Djurovich, D. Murphy, F. Abdel-Razzaq, R. C. Kwong, I. Tysba, M. Bortz, B. Mui, R. Bau, M. E. Thompson, *Inorg. Chem.* **2001**, *40*, 1704–1711; b) C. Adachi, M. A. Baldo, S. R. Forrest, S. Lamansky, M. E. Thompson, R. C. Kwong, *Appl. Phys. Lett.* **2001**, *78*, 1622–1624; c) J. Nishida, H. Echizen, T. Iwata, Y. Yamashita, *Chem. Lett.* **2005**, *34*, 1378–1379.

[4] P. Coppo, E. A. Plummer, D. De Cola, *Chem. Commun.* **2004**, 1774–1775.

[5] a) A. Beeby, S. Bettington, I. D. W. Samuel, Z. Wang, *J. Mater. Chem.* **2003**, *13*, 80–83; b) C. H. Yang, C. C. Tai, I. W. Sun, *J. Mater. Chem.* **2004**, *14*, 947–950; c) S. Jung, Y. Kang, H.-S. Kim, Y.-H. Kim, C.-L. Lee, J.-J. Kim, S.-K. Lee, S.-K. Kwon, *Eur. J. Inorg. Chem.* **2004**, 3415–3423; d) B. Liang, C. Jiang, Z. Chen, X. Zhang, H. Shi, Y. Cao, *J. Mater. Chem.* **2006**, *16*, 1281–1286; e) Z. Liu, M. Guan, Z. Bian, D. Nie, Z. Gong, Z. Li, C. Huang, *Adv. Funct. Mater.* **2006**, *16*, 1441–1448.

[6] a) Md. K. Nazeerudin, R. Humphry-Baker, D. Berner, S. Rivier, L. Zuppiroli, M. Grätzel, *J. Am. Chem. Soc.* **2003**, *125*, 8790–8797; b) C. Lee, R. R. Das, J. Kim, *Chem. Mater.* **2004**, *16*, 4642–4646; c) J. Li, P. I. Djurovich, B. D. Alleyne, M. Yousufuddin, N. N. Ho, J. C. Thomas, J. Peters, R. Bau, M. E. Thompson, *Inorg. Chem.* **2005**, *44*, 1713–1727.

[7] a) M. A. Baldo, M. E. Thompson, S. R. Forrest, *Nature* **2000**, *403*, 750–753; b) S. Lamansky, P. Djurovich, D. Murphy, F. Abdel-Razzaq, H.-E. Lee, C. Adachi, P. E. Burrows, S. R. Forrest, M. E. Thompson, *J. Am. Chem. Soc.* **2001**, *123*, 4304–4312; c) I. R. Laskar, T.-M. Chen, *Chem. Mater.* **2004**, *16*, 111–117; d) Review: E. Holder, B. M. W. Langeveld, U. S. Schubert, *Adv. Mater.* **2005**, *17*, 1109–1121; e) *Organic Electroluminescence* (Ed.: Z. H. Kafafi), CRC Press, Boca Raton, **2005**; f) D. F. Perepichka, H. Meng, M.-M. Ling in *Organic Light-Emitting Materials and Devices* (Eds.: Z. Li, H. Meng), CRC Press, Boca Raton, **2006**, pp. 413–449; g) P.-T. Chou, Y. Chi, *Chem. Eur. J.* **2007**, *13*, 380–395.

[8] a) E. A. Plummer, J. A. Hofstraat, L. De Cola, *Dalton Trans.* **2003**, 2080–2084; b) J. D. Slinker, A. A. Gorodetsky, M. S. Lowry, J. Wang, S. Parker, R. Rohl, S. Bernhard, G. G. Malliaras, *J. Am. Chem. Soc.* **2004**, *126*, 2763–2767; c) M. Lepeltier, T. K.-M. Lee, K. K.-W. Lo, L. Toupet, H. L. Bozec, V. Guerchais, *Eur. J. Inorg. Chem.* **2005**, 110–117; d) J. I. Goldsmith, W. R. Hudson, M. S. Lowry, T. H. Anderson, S. Bernhard, *J. Am. Chem. Soc.* **2005**, *127*, 7502–7510; e) F. Neve, M. La Deda, A. Crispini, A. Bellusci, F. Puntoriero, S. Campagne, *Organometallics* **2004**, *23*, 5856–5863; f) Review: M. S. Lowry, S. Bernhard, *Chem. Eur. J.* **2006**, *12*, 7970–7977; g) Review: J. D. Slinker, J. Rivnay, J. S. Moskowitz, J. B. Parker, S. Bernhard, H. D. Arbruña, G. G. Malliaras, *J. Mater. Chem.* **2007**, *17*, 2976–2988.

[9] a) B. Tamayo, S. Garon, T. Sajoto, P. I. Djurovich, I. M. Tsyba, R. Bau, M. E. Thompson, *Inorg. Chem.* **2005**, *44*, 8723–8732; b) Q. Zhao, S. Liu, M. Shi, C. Wang, M. Yu, L. Li, F. Li, T. Yi, C. Huang, *Inorg. Chem.* **2006**, *45*, 6152–6160; c) M. S. Lowry, W. R. Hudson, R. A. Pascal, Jr., S. Bernhard, *J. Am. Chem. Soc.* **2004**, *126*, 14129–14135.

[10] Recently a homoleptic complex $(C^\wedge N^+)_3Ir(PF_6^-)_3$ with phenylpyridine ligands bearing a charged peripheral tributylphosphonium group has been studied: H. J. Bolink, L. Cappelli, E. Coronado, A. Parham, P. Stössel, *Chem. Mater.* **2006**, *18*, 2778–2780.

[11] a) J. I. Kim, I.-S. Shin, H. Kim, J.-K. Lee, *J. Am. Chem. Soc.* **2005**, *127*, 1614–1615; b) P. M. Griffiths, F. Loiseau, F. Puntoriero, S. Serroni, S. Campagna, *Chem. Commun.* **2000**, 2297–2298; c) K. K.-W. Lo, C.-K. Chung, T. K.-M. Lee, L.-H. Lui, K. H.-K. Tsang, N. Zhu, *Inorg. Chem.* **2003**, *42*, 6886–6897; d) H. J. Bolink, L. Cappelli, E. Coronado, M. Grätzel, E. Orti, R. D. Costa, P. M. Viruela, Md. K. Nazeerudin, *J. Am. Chem. Soc.* **2006**, *128*, 14786–14787.

[12] a) H. Zhen, C. Jiang, W. Yang, J. Jiang, F. Huang, Y. Cao, *Chem. Eur. J.* **2005**, *11*, 5007–5016; b) J. Jiang, C. Jiang, W. Yang, H. Zhen, F. Huang, Y. Cao, *Macromolecules* **2005**, *38*, 4072–4080; c) C. S. M.

 © 2008 Wiley-VCH Verlag GmbH & Co. KGaA, Weinheim

Mak, A. Hayer, S. I. Pascu, S. E. Watkins, A. B. Holmes, A. Köhler, R. H. Friend, *Chem. Commun.* **2005**, 4708–4710.
[13] a) M. Tavasli, S. Bettington, M. R. Bryce, H. Al Attar, F. B. Dias, S. King, A. P. Monkman, *J. Mater. Chem.* **2005**, *15*, 4963–4970; b) H. Al Attar, A. P. Monkman, M. Tavasli, S. Bettington, M. R. Bryce, *Appl. Phys. Lett.* **2005**, *86*, 121101; c) S. Bettington, M. Tavasli, M. R. Bryce, A. S. Batsanov, A. L. Thompson, H. A. Al Attar, F. B. Dias, A. P. Monkman, *J. Mater. Chem.* **2006**, *16*, 1046–1052; d) S. Bettington, M. Tavasli, M. R. Bryce, A. Beeby, H. Al Attar, A. P. Monkman, *Chem. Eur. J.* **2007**, *13*, 1423–1431.
[14] a) J. C. Ostrowski, M. R. Robinson, A. J. Heeger, G. C. Bazan, *Chem. Commun.* **2002**, 784–785; b) X. Gong, W. Ma, J. C. Ostrowski, K. Bechgaard, G. C. Bazan, A. J. Heeger, D. Moses, *Adv. Funct. Mater.* **2004**, *14*, 393–397; c) A. J. Sandee, C. K. Williams, N. R. Evans, J. E. Davies, C. E. Boothby, A. Köhler, R. H. Friend, A. B. Holmes, *J. Am. Chem. Soc.* **2004**, *126*, 7041–7048; d) W.-Y. Wong, G.-J. Zhou, X.-M. Yu, H.-S. Kwok, B.-Z. Tang, *Adv. Funct. Mater.* **2006**, *16*, 838–846; e) W.-Y. Wong, G.-J. Zhou, X.-M. Yu, H.-S. Kwok, Z. Lin, *Adv. Funct. Mater.* **2007**, *17*, 315–323.
[15] D. Tzalis, Y. Tor, S. Failla, J. S. Siegel, *Tetrahedron Lett.* **1995**, *36*, 3489–3490.
[16] N. Miyaura, A. Suzuki, A. *Chem. Rev.* **1995**, *95*, 2457–2483.
[17] A. L. Kanibolotsky, R. Berridge, P. J. Skabara, I. F. Perepichka, D. C. C. Bradley, M. Koeberg, *J. Am. Chem. Soc.* **2004**, *126*, 13695–13702.
[18] S. Sprouse, K. A. King, P. J. Spellane, R. J. Watts, *J. Am. Chem. Soc.* **1984**, *106*, 6647–6653.
[19] F. Neve, A. Crispini, S. Campagna, S. Serroni, *Inorg. Chem.* **1999**, *38*, 2250–2258.
[20] a) F. Neve, A. Crispini, *Eur. J. Inorg. Chem.* **2000**, 1039–1043; b) K. K.-W. Lo, C.-K. Chung, N. Zhu, *Chem. Eur. J.* **2003**, *9*, 475–483; c) K. K.-W. Lo, J. S.-W. Chan, C.-K. Chung, V. W.-H. Tsang, N. Zhu, *Inorg. Chim. Acta* **2004**, *357*, 3109; d) K.-M. Cheung, Q.-F. Zhang, K.-W. Chan, M. H. W. Lam, I. D. Williams, W.-H. Leung, *J. Organomet. Chem.* **2005**, *690*, 2913–2921.
[21] K. K.-W. Lo, C.-K. Chung, N. Zhu, *Chem. Eur. J.* **2006**, *12*, 1500–1512.
[22] A. Hazell, *Polyhedron* **2004**, *23*, 2081–2083.
[23] N. G. Connelly, W. E. Geiger, *Chem. Rev.* **1996**, *96*, 877–910.
[24] F. Neve, A. Crispini, S. Serroni, F. Loiseau, S. Campagna, *Inorg. Chem.* **2001**, *40*, 1093–1101.
[25] B. E. Koene, D. E. Loy, M. E. Thompson, *Chem. Mater.* **1998**, *10*, 2235–2250.
[26] S.-J. Liu, Q. Zhao, R.-F. Chen, Y. Deng, Q.-L. Fan, F.-Y. Li, L.-H. Wang, C.-H. Huang, W. Huang, *Chem. Eur. J.* **2006**, *12*, 4351–4361.
[27] J. N. Demas, G. A. Crosby, *J. Phys. Chem.* **1971**, *75*, 991–1024.
[28] A. Tsuboyama, H. Iwawaki, M. Furugori, T. Mukaide, J. Kamatani, S. Igawa, T. Moriyama, S. Miura, T. Takiguchi, S. Okada, M. Hoshino, K. Ueno, *J. Am. Chem. Soc.* **2003**, *125*, 12971–12979.

Received: February 23, 2007
Revised: August 17, 2007
Published online: November 21, 2007

 © 2008 Wiley-VCH Verlag GmbH & Co. KGaA, Weinheim